

TUNING ELECTRICAL AND THERMAL CONNECTIVITY IN MULTIWALLED CARBON NANOTUBE BUCKYPAPER

Keqin Yang, Jian He, Pooja Puneet, Malcolm J. Skove, Terry M. Tritt and Apparao M. Rao

Department of Physics and Astronomy, Clemson University, Clemson, SC 29634-0978

Introduction

Even though the individual carbon nanotube (CNT) exhibits extraordinary high electrical conductivity, the inter-tube interaction has been proposed as the dominant factor governing the electrical transport in a CNT network [1,2]. Some mechanical or chemical methods have been developed to modify the tube junctions in the CNT network, such as arranging the orientation of CNTs or acid treatment. But these methods either need multi steps or special morphology of the nanotubes [2,3]. In our early work, we have shown that the Spark Plasma Sintering (SPS) process can modify the tube-tube contacts and induce covalent inter-tubular bonding in aligned multi walled carbon nanotubes (MWCNTs) resulting in enhanced electrical conductivity in the transverse direction; with the transverse electrical conductivity in SPS-ed sample being slightly higher than the longitudinal electrical conductivity [4]. In this study, we find that the micro-morphology, as well as the electrical and thermal connectivity of MWCNTs in the buckypaper (BP) can be tuned simply by controlling one parameter, viz., the SPS temperature.

Experimental

The MWCNT-BP (thickness ~ 0.3 mm) used in this study are provided by Nano TechLabs, Inc. and all the samples were obtained from a single BP sheet. For transport measurements, thick samples were prepared by stacking six pieces of this BP (diameter ~ 1.2 cm) inside a graphite die (bore diameter ~ 1.2 cm) and subjecting them to the SPS process (Model Dr. Sinter 1020, Sumitomo Coal Mining CO., Ltd., Japan). A constant pressure of ~ 7 MPa was maintained in all SPS experiments while the applied current density was varied to attain different SPS temperatures (T_{SPS}). We sintered the stack of BPs at 500, 800, 900, 1000, 1200 and 1500 °C in vacuum. These samples are hereafter referred to S500 S800, S900, S1000, S1200 and S1500, respectively. The densities of samples were measured as m/V (m is mass and V is volume). Field emission scanning electron microscope (FESEM, Hitachi® S4800) and high resolution transmission electron microscopy (HRTEM, Hitachi® TEM 9500) were used to examine the micro-morphology before and after the SPS process.

Strips with typical dimensions of $5 \times 2 \times t$ mm³ (t is the thickness of the sample, which depends on the density of the samples) were cut from each sintered sample. The DC electrical resistivity (ρ), thermoelectric power (S) and thermal conductivity (κ) of the strips were measured in the temperature

range from 10 to 300 K. For ρ and κ measurements, a conventional 4-probe configuration was adopted. In all transport measurements, silver paint was used to form ohmic contacts.

Results and Discussion

The FESEM images in figures 1(a)-(d) show that the SPS process tends to pack MWCNTs together while largely preserving individual tubular micro-morphology. The as-prepared BP (referred as AP) is composed of randomly oriented MWCNTs with a dominant tube diameter of ~ 30 nm and no preferred orientation. Local welding of MWCNTs (inter-tube bonds) has been found in samples subjected to $T_{SPS} > 1000$ °C. The increase in density of the MWCNT BP is approximately linearly in T_{SPS} as shown in Fig. 1 (e). The density of S1500 sample is about 3 times that of the AP sample. Room temperature values of ρ and κ for the SPS-ed samples are plotted as a function of packing density in figure 1(h). Clearly, ρ (κ) decreases (increases) monotonically with increasing packing density.

The temperature dependence of resistivity (ρ) for the SPS-ed MWCNT-BP samples is shown in figure 2(a). For convenience, we designate the AP sample with a pseudo-SPS temperature of 25 °C. The overall magnitude of ρ systematically decreases with increasing T_{SPS} over the temperature range studied, saturating in samples that were SPS-ed at $T \geq 1200$ °C. The S1500 sample showed the lowest room temperature $\rho \sim 0.008$ Ω -cm which is comparable to that reported in disordered individual MWCNTs.

Figure 2b depicts the relation between room temperature resistivity (ρ_{RT}) and T_{SPS} . The relation can be well described by a power law behavior, confirming a percolation-type behavior. A standard percolation model predicts that the connection-dependence of resistivity is [5]

$$\rho \propto (N - N_C)^{-\alpha} \approx (T_{SPS} - T_{Th})^{-\alpha} \quad (1)$$

Here, N is the number of inter-tube connections and N_C is the threshold value. The power law behavior should hold in the vicinity of the threshold, in which the exponent α depends only on the dimensionality of the system. Theory predicts $\alpha = 1.33$ for 2-D systems [5]. The inset in figure 2(b) shows the fitting to the data in the 500-1500 °C range to equation (1). As we did not observe a discernable change in ρ for $T_{SPS} < 500$ °C, it is plausible to assume a threshold value $T_{Th} \approx 500$ °C. The best fitting yields a value of $\alpha = 1.3$.

$\rho(T)$ for all samples shows a non-metallic behavior, which we assume to arise from the inter-tube junctions. At each junction, the localized defects establish an energetic barrier which the carriers overcome via hopping or tunneling [6]. This gives rise to the strong temperature dependence in $\rho(T)$ at low temperatures.

Interestingly, a plateau in $\rho(T)$ is evident in the S1500 sample between 20-50 k. In the same temperature range, a phonon drag peak present in thermoelectric power (S) [4, 7, 8] suggesting that the observed signatures in $\rho(T)$ and $S(T)$ in the S1500 sample are most probably due to a unified mechanism, e.g.[9, 10], the electron phonon coupling. $S(T)$ exhibits a

positive slope and is linear in T for most of the temperature range, signifying the metallic nature of MWCNTs (Fig. 2 (c)). The magnitude of $S(T)$ and dS/dT changes monotonically with increasing T_{SPS} except for the S900 sample (inset of Fig 2 (c)). Since the $S(T)$ is sensitive to the Fermi surface topology, the variation of dS/dT with T_{SPS} reflects the systematic change of Fermi surface [9].

The magnitude of thermal conductivity (κ) increases systematically with increasing T_{SPS} , and all $\kappa(T)$ curves increase monotonically with temperature (Fig.2 (d)). The electron contribution for $\kappa(T)$ is less than 1% for all the samples over the entire temperature range estimated from the Wiedemann-Franz relationship. If we use $\kappa \sim T^\gamma$ to fit $\kappa(T)$ for different samples below 120 K, γ increases monotonically with T_{SPS} from nearly 1 to 2 (the inset of Fig. 2 (d)). Given the high Debye temperature of CNT [11], the wavelength of active phonons are thus much larger than the characteristic size of a junction, so the phonons probe the thermal connectivity (dimensionality) of the MWCNT-BP while they are less affected by the detailed nature of inter-tube junctions. This implies the thermal connectivity crosses from a 1-D character (in the AP sample) to a higher dimensional character (in other SPS-ed samples) [12]. The increasing γ values clearly indicate an enhanced thermal connectivity in the system with increasing T_{SPS} .

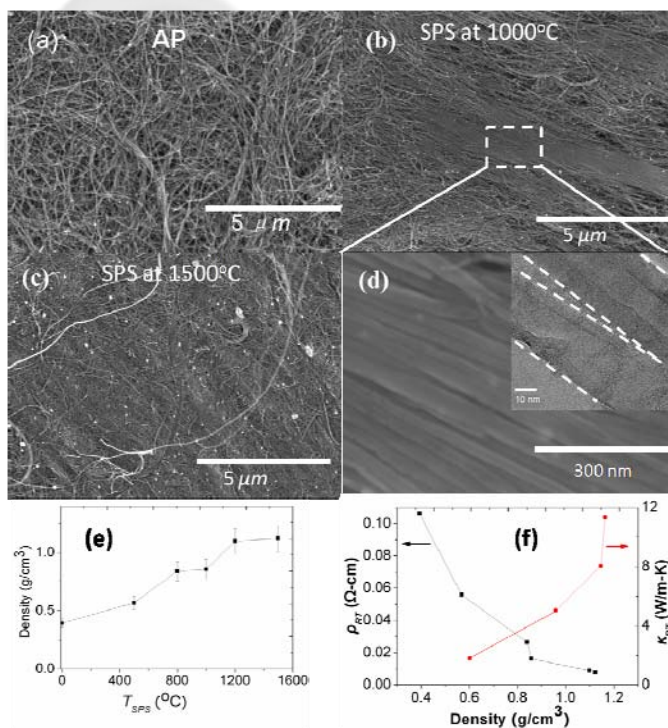


Fig. 1 SEM images of samples. (a) as prepared, (b) S1000 (b), and S1500 (c), and S1500. Panels (d) represent higher magnification images of (b). Inset in (d) is a representative HRTEM image of the S1000 sample in which MWNTs are found welded together. In panel (e), the density of MWCNT-BP is plotted as a function of T_{SPS} (error bar $\sim \pm 10\%$).

Room temperature values of ρ and κ for the SPS-ed samples are plotted as a function of packing density (panel f).

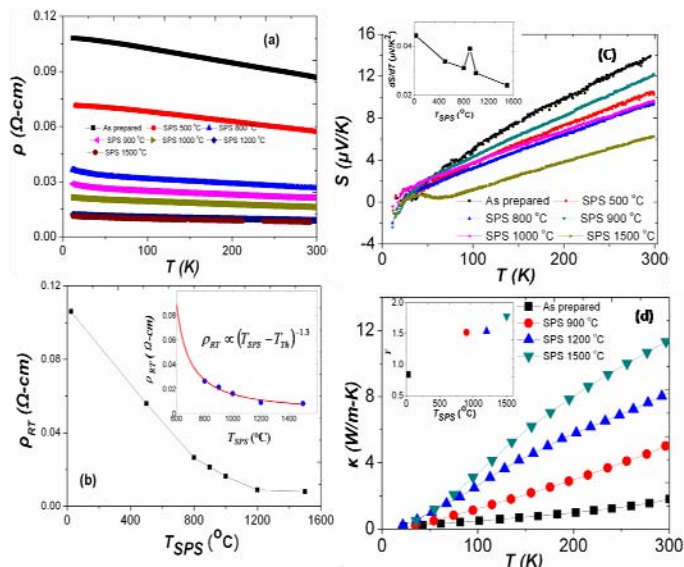


Fig. 2 Plots of $\rho(T)$ (a), $S(T)$ (c) and $\kappa(T)$ (d) of MWCNT-BP sintered at different T_{SPS} (a), and ρ_{RT} vs T_{SPS} (b). The inset in (b) shows the best fit power law behavior (cf. equation (1)), indicating a percolation-type nature for the samples. The inset in (c) shows the slope of $S(T)$ above 100 K. We fit $\kappa(T)$ below 120 K to the formula $\kappa \sim T^\gamma$, the relationship between T_{SPS} and γ is shown in inset of (d).

Conclusions

The electrical conductance of MWCNT-BP is governed by the inter-tube junctions and exhibits a percolation-type behavior. With increasing T_{SPS} , an increasing number of junctions are formed. In the sample SPS-ed at 1500 °C, the phonon drag effect causes a plateau in $\rho(T)$ and a hump in $S(T)$. The long wavelength phonons are less affected by the detailed nature of junctions, so that they simply probe the connectivity of the MWCNTs (dimensionality). With increasing T_{SPS} , the thermal conductivity crosses to a higher dimensionality.

References

- [1] Dresselhaus M S, Dresselhaus and G, Eklund P C *Science of Fullerenes and Carbon Nanotubes* (San Diego: Academic) 1996
- [2] Nirmalraj P N, *et al.*, 2009 *Nano Lett.* **9** 3890
- [3] Wang D, *et al.*, 2008 *Nanotechnology* **19** 075609
- [4] Keqin Y., *et al.*, 2010 *Carbon* **48** 756
- [5] Stauffer G 1985 *Introduction to Percolation Theory* (London: Taylor & Francis)
- [6] Kaiser A B, *et al.*, 1998 *Phys Rev B* **57** 1418
- [7] Sugihara K, *et al.*, 1977 *J. Phys. Soc. Jpn* **43** 1644
- [8] Ayache C, *et al.*, 1980 *Phys. Rev. B* **21** 2462
- [9] Scarola V W *et al.*, 2002 *Phys. Rev. B* **66** 205405
- [10] Vavro J, *et al.*, 2003 *Phys. Rev. Lett.* **90** 065503
- [11] Hone J 2004 *Carbon Nanotube: Thermal Properties* Dekker Encyclopedia of Nanoscience and Nanotechnology 603
- [12] Li W, *et al.*, 1999 *Phys. Rev. B* **59** R9015